Effect of the finite extensibility of polymer chains and of the finite size of added electrolyte ions on polyelectrolyte brushes

Sanjay Misra and Sasidhar Varanasi
Department of Chemical Engineering, University of Toledo, Toledo, Ohio 43606

Our earlier polyelectrolyte brush theory [Macromolecules **22**, 4173 (1989)] was derived by equating the sum of the nonelectrostatic and electrostatic potentials of the polymer segment to an overall parabolic potential shown to exist in the brush by Milner, Witten, and Cates (MWC) [Macromolecules **21**, 2610 (1988)]. Here we correct the theory to take into account the finite extensibility of the chains by adopting the non-Gaussian stretch (or entropy) term of Shim and Cates [J. Phys. France **50**, 3535 (1989)]. This correction leads to brush heights which will never exceed the chain length; an aspect that was not accounted for in the earlier work of MWC. In addition, the ions of the added symmetric electrolyte are considered to be hard spheres, the size of the cation and anion assuming different values in general. The total electrochemical potential of the ions, therefore, includes a volume exclusion term as well. The ions are assumed to "view" the solvent as a continuum (characterized only by its dielectric constant) and the brush layer as an obstacle course of randomly distributed spherical hard segments. The treatment is made simple by assuming a regime where the volume fraction of ions is much lower than the segment or solvent volume fractions.

I. INTRODUCTION

If polymer molecules are terminally attached (or grafted) to a surface in high density, they tend to form dense and extended surface layers called brushes. "High density" is attained when the spacing of the graft points on the surface is much smaller than the end to end distance of a free polymer chain. Each chain, under these conditions, is forced (or stretched) away from the surface due to excluded volume (or electrostatic) repulsions from the multitude of surrounding chains. In practice, brushes can be produced by chemically attaching one end of the polymer chain to an active group on the substrate surface.[1] If the polymer (or polyelectrolyte) and the surface are incompatible, then in a good solvent (or a medium with lower ionic strength) the grafted chains will repel each other and form brushes. The same effect can also be realized by adsorbing di-block copolymers, one of whose blocks has no affinity for the solvent while the other is soluble.[2] Thus, the soluble block will stretch away from the surface, being anchored there by the block which has no affinity for the solvent. Finally, graft copolymers resembling combs may also be used to form brushes.[3] In this case, of course, the backbone of the "comb" is adsorbed onto the surface while the "teeth" (or the side chains) stretch away into the solution. Grafting density is determined by the density of active surface groups in the case of grafted polymers, by the relative lengths of the blocks in the case of copolymer adsorption or the proportion of the side chains in graft copolymers. Polymer brushes, and the principles underlying their description, find applications in areas as diverse as colloid stabilization,[4-6] alteration of microporous membranes,[7,8] adhesion,[11,12] di-block copolymer (macrosurfactant) micelles,[9,10] etc. The conformational characteristics of the so-called brushes have been approached from varying view points by many investigators. These include the scaling arguments of Alexander[13] and de-Gennes,[14] lattice mean field approach of Cosgrove et al.[15] Monte Carlo simulations of S. Hirz[16] and the continuum mean field picture of Ho and Muthukumar[17] and Milner, Witten, and Cates (MWC).[18]

The approach of MWC is particularly appealing since, for the case of monodisperse chains, they predict a simple, parabolically decaying segment potential profile away from the surface. Using an appropriate equation of state, which relates the local segment volume fraction to the segment chemical potential, one can deduce the segment density profile in the polymer brush. This approach has recently been extended by Miklavic and Marcelja[19] and Misra et al.[20] to polyelectrolytes as well, by equating the total electrochemical segment potential to the overall parabolic potential and solving the coupled Poisson–Boltzmann equation.

However, as noted by MWC,[18] the parabolic potential would not be valid for very highly stretched chains (for example, when the end to end chain distance approaches the chain length). As discussed in the next section, this is due to the limitations upon the stretch (or entropy) part of the chain free energy representation adopted in their work. In fact, the parabolic potential can lead to predictions of brush height in excess of the polymer chain length, when interchain and intrachain repulsions are high. As Shim and Cates[21] point out, in order to obtain physically meaningful results, therefore, the representation of the free energy of the chain needs a constraint on the stretching of the polymer chain. The constraint limits the maximum end to end distance of the chain to the length of the chain or, in other words, ensures that the polymer chains are only *finitely extensible*. This is an important caveat for polyelectrolytes which can become very highly stretched with increasing backbone charge or decreasing ionic strength of the surrounding solution.

One other parameter that has not been accounted for

earlier is the finite size of the ions of the added electrolyte. In polymer brushes (or near the surface in the case of homopolymer adsorption) the polymer segment density is very high. If the polymer density is high enough, the intersegmental spacing would become of the same order as the ion size. In this case, we would expect the mobile ions and the polymer segments to have an excluded volume type of interaction. The free energy of the mobile ions would therefore include a nonelectrostatic energy, due to volume exclusion, in addition to the electrostatic energy. The local concentration of the ions would therefore depend not only upon the electrostatic potential but also on the local segment concentration. The shielding of the electrostatic interactions between the segments, and consequently the segment density distribution (SDD), in turn depends upon the local ion concentration. It is, therefore, important to account for the finite size of the mobile ions.

We present here these two corrections to our polyelectrolyte brush theory[20] arising from the *finite extensibility* of the polymer chains and *finite size of the mobile electrolyte ions*. The next two sections address these effects individually. These corrections are then incorporated into the earlier polyelectrolyte brush theory and the resulting model is presented. Finally, predictions for segment density distributions, brush heights, and free energy are presented and discussed.

II. FINITE EXTENSIBILITY

The free energy of adding the ith chain to the brush (or the action of the chain) can be written as follows:

$$S_i = \int_0^N \{T_i[\mathbf{r}(s)] + W_i[\mathbf{r}(s)]\}ds. \tag{1}$$

Here S_i is the action of a chain containing N statistical segments. The integral over the contour (s being the ranking of the segment from one end, say the free end) sums up the free energy of each segment (the entropy or stretch term T and the interaction potential W). The trajectory of a chain is given by a set of coordinates $\mathbf{r}_i(s)$, denoting the position of the sth segment on the ith chain. In the case of a uniform surface layer, one can replace the the vector $\mathbf{r}_i(s)$ with the single coordinate perpendicular to the surface, $x_i(s)$. We assume hereafter that x is dedimensionalized by the segment length, a and that S, T, W, etc. are dedimensionalized by the factor (kT_s), k being the Boltzmann constant and T_s the absolute temperature. In the previous self-consistent-field (SCF) theory, MWC assumed the following form for the stretch energy:[18]

$$T_i(s) = \tfrac{1}{2}\left[\frac{dx_i(s)}{ds}\right]^2 = \tfrac{1}{2}\dot{x}_i^2. \tag{2}$$

With this substitution for T_i, the single chain action of Eq. (1) resembles the action of a particle of unit mass traveling with a velocity dx_i/ds in an inverted potential W, s playing the role of "time".

Now, the step-function ansatz of Alexander[13] and de-Gennes[14] yields that the equilibrium brush height h^* scales linearly with chain length ($h^* \sim N$), i.e., the chains are highly stretched. Thus, while the end to end distance of the chains scale as N, the fluctuations around it scale as $\sim N^{3/5}$.

MWC therefore conclude that, for very long chains ($N^{3/5} \ll N$), only those conformations which correspond to the trajectories of classical particles are important (for further details, see Ref. 18), i.e., only these paths contribute to the brush properties. These are, of course, paths with the minimum free energy for given chain-end locations. All chains end at the surface [$x_i(N) = 0$] and their free ends have no external force on them ($dx_i(0)/ds = 0$). Thus, chain conformations are analogous to the trajectories of *Newtonian* particles starting with a zero velocity somewhere in the brush and ending at the surface. Also, if all chain lengths are equal then, in the analogous classical mechanics picture, no matter where the trajectories of these classical particles start, they all take the same time to end up at the surface. Thus, as pointed out by MWC, the potential in the brush is that of a harmonic oscillator, i.e., parabolic. The equal time potential, W, is therefore given as

$$W(x) = A - Bx^2, \tag{3}$$

where, $B = \pi^2/8N^2$ and A is a constant which only depends upon the brush height. One can now use a suitable equation of state, to establish a relation between the local segment density and W, and compute a segment density profile.

The classical mechanics analogy and the parabolic potential result, however, from adopting a particular form (also called the Gaussian form) for the stretch energy [Eq. (2)]. This form is valid only when stretch rates are low (for example, see the derivation by de Gennes[22]) and would break down as the polymer chains become more and more extended, as noted by MWC. In fact, it can be argued, that, by definition, the chains in a brush *have to be* highly stretched and therefore corrections to the Gaussian stretch energy are necessary almost throughout the brush forming regime. Without these corrections, a parabolic potential could predict brush heights in excess of the chain length (for high grafting densities and high excluded volume interactions or for large electrostatic repulsions in polyelectrolytes), which physically is not possible. Thus, the correction to the stretching term should be of a form that will limit the stretching rate, dx_i/ds, to 1.

The recent work of Shim and Cates[21] addresses this problem of finite extensibility and the salient features of their approach are recounted below briefly. Of course, once the stretching correction has been incorporated, one can again invoke the earlier arguments to show that only the minimum free energy paths are important. In the case of grafted chains of equal length, one obtains, once again, an equal time potential—which in general is not a parabola. As Shim and Cates point out, the correction for the stretch term, while different for different polymers must have the following property. At low stretching rates, one should recover the Gaussian stretch form while the derivative of the stretching term with respect to the stretch rate should diverge as the stretch rate approaches unity. In other words,

$$\dot{x} \to 0, \quad T \to \frac{\dot{x}^2}{2}, \tag{4a}$$

$$\dot{x} \to 1, \quad \frac{\partial T}{\partial \dot{x}} \to \infty. \tag{4b}$$

To illustrate how these constraints lead to the proper equal time potential, consider the constant of motion, H, of the polymer chain. This is analogous to the total energy of a classical particle (moving under the influence of conservative forces) which has to remain constant. H can also be visualized as the interaction potential (potential energy of particle) of the free segment ($s = 0$) which has no stretch (kinetic) energy. Using the classical mechanics analogy, this constant of motion (or energy) may be written as

$$H = \dot{x}\frac{\partial L}{\partial \dot{x}} - L, \quad \text{where } L(\dot{x},x,s) = T + W, \quad (5)$$

L being the Lagrangian.

Thus, since $\partial T/\partial x$ diverges as $\dot{x} \to 1$, the total energy of the chain (particle) also diverges as $\dot{x} \to 1$. This has the effect of forcing H to behave as follows:

$$\dot{x} \to 0, \quad H \sim \frac{\dot{x}^2}{2} + W \quad \text{(Newtonian particle)} \quad (6a)$$

$$\dot{x} \to 1, \quad H \to \infty \quad (6b)$$

Thus, in order that the chains in the brush have a finite free energy, no chain can have local stretch rates of unity. The constraints of Eq. (4) thus have the effect of making the potential steep and divergent as the brush height approaches the chain length, N. The predicted brush heights are therefore less than the chain length and hence more realistic. Shim and Cates have outlined an approach whereby, at least in principle, one can obtain equal time potentials for various functions, T. A brief account of this approach is given in the Appendix (further details can be found in Ref. 21). They have obtained an analytical expression for the potential if the stretch term has the following form:

$$T = \frac{\dot{x}^2}{2(1 - |\dot{x}|)}. \quad (7)$$

This function proves to be mathematically tractable and they show that

$$W(x) = A(h) - U(x), \quad (8)$$

where A is a constant depending only upon the brush height h and

$$x(U) = N\beta \left\{ 2\sqrt{\frac{U}{\pi}} - \frac{2}{\beta} \int_0^{\beta\sqrt{U}} dy\, y \exp(y^2)\mathrm{erfc}(y) \right\}, \quad (9)$$

where, $\beta = (2/\pi)^{1/2}$.

It is easily verified that this potential, $U(x)$, diverges as $x \to N$. It can be noticed that by dropping the second term of the right-hand side of Eq. (9), one recovers the earlier parabolic potential. In fact, near the surface the potential starts off as a parabola and becomes progressively steeper. The second term is the correction for finite extensibility that causes the potential to drop steeper and forces it to diverge at $x = N$.

As pointed out earlier, this potential is not general since the finite extensibility correction of Eq. (7) is not general. However, the *nonparabolic* potential of Shim and Cates is an excellent analytical result which serves to illustrate the importance of accounting for finite extensibility corrections. As we shall see, these corrections are especially important

for polyelectrolyte brushes where electrostatic repulsions among chains cause them to be highly stretched.

III. FINITE SIZE OF THE ELECTROLYTE IONS

In the previous study on polyelectrolyte brushes,[20] the finite size of the ions was not taken into account. The electrochemical potential of the ions was therefore independent of their size and their local concentration depended upon the local electrostatic potential as follows:

$$n_i = n_i^\infty \exp\left(-\frac{Z_i e\Psi}{kT_s}\right), \quad (10)$$

where n_i is the local number density of ions of the ith kind and n_i^∞ is their corresponding bulk concentration. Also, Z_i is the valence of these ions, e the protonic charge, and Ψ the local electrostatic potential.

In fact, however, even if the ions are assumed to be point charges, the space occupied by the polymer segments is excluded to them. Thus, if the polymer volume fraction were unity, one expects the ions to be completely excluded from the brush region ($n_i = 0$). Equation (10), nevertheless, would predict a finite charge density, which cannot be true. In practice, though, the mobile ions have a finite size which hinders their ability to penetrate into the dense brush (or dense regions in homopolymer layers as well). In other words, these ions experience excluded volume kinds of interactions with the polymer segments. Therefore, even if the polymer volume fraction were not too high, the effect of exclusion would be felt for ions with a finite size. The effect of this exclusion would be especially important if the size of the mobile ions became comparable with the spacing of the segments inside the layer.

In order to correct Eq. (10), to incorporate the above, it is useful to visualize any location within the brush region as a porous medium composed of polymer segments into which the electrolyte ions are partitioning from the bulk solution. In particular, one can consider the brush to be composed of hard spherical segments which are randomly placed, the voidage between the segments being equivalent to pores. This visualization, in addition to being realistic, has the advantage that the rigourous results for partitioning of hard spheres (in the present case the ions) into such porous media are now available.[23] One can use the following simple argument to appreciate the fact that in a typical brush the characteristic size of the voidage is comparable to the size of the ions. A characteristic void dimension, r_p, can defined as

$$r_p = \frac{\text{Void Volume, } V}{\text{Void Surface Area, } S} = \frac{a(1 - \Phi)}{6\Phi}. \quad (11)$$

Let the radius of the ith ion be r_i. One can now define a quantity λ_i to denote the size of the ion relative to the segment spacing, r_p.

$$\lambda_i = \frac{6\Phi r_i}{a(1 - \Phi)}. \quad (12)$$

One can expect the excluded volume interactions to play an appreciable role for $\lambda \geqslant 0.1$. Using some typical values for segment volume fraction, Φ (~ 0.25) and the segment diameter, a (~ 1 nm), it can be verified that all ions of size greater

than 0.05 nm (0.5 Å) will have significant excluded volume interactions with the polymer layer. Most effective ionic radii, in aqueous media, range from 0.2–1 nm[24] (see, for example, Table 1.3, Ref. 24). One expects, therefore, that the finite size of the ions would play an important role in their concentration distribution. The ion distribution, in turn, affects the electrostatic screening of segment charges and hence the segment density distribution, Φ.

A realistic expression for the ionic concentrations inside the voidage may be written as follows:

$$n_i^p = n_i^\infty f_i(\hat{r}_i,\ldots,\ \hat{r}_j,n_i^\infty,\ldots,\ n_j^\infty)\exp\left\{-\frac{Z_i e\Psi + g_i(\Phi,\hat{r}_i)}{kT_s}\right\},$$

(13)

where g_i is the difference in the standard state chemical potential of the ith ion in the void space and in the bulk. It can also be visualized as the free energy associated with excluded volume interaction of the ion with the polymer. n_i^p is the local concentration of the ith ion in the void space (number of ions per unit void volume). f_i is the ratio of the activity coefficients for the ith ion in the void space and the bulk. $\hat{r}_i,\ldots,\hat{r}_j$, are the ratio of the respective ion radii to the segment radius ($\hat{r}_i = 2r_i/a$), and $n_i,\ldots,n_j$, the local concentrations of the respective ions.

In the Henry law regime (where ionic concentrations are low enough for ion–ion hard core interactions to be unimportant), the ratio of the activity coefficients, f_i, tends towards unity. Therefore, the expression for the concentration of the ith ion inside the voidage can be represented as

$$\frac{n_i^p}{n_i^\infty} \equiv K_e K_n,$$

(14a)

where K_e and K_n can be visualized as the contributions to the overall partitioning coefficient of the ions between the brush and the bulk phase, stemming from electrostatic and hard sphere interactions, respectively. Clearly,

$$K_e = \exp\left(-\frac{Z_i e\Psi}{kT_s}\right),$$

(14b)

and

$$K_n = \exp\left(-\frac{g_i(\Phi,\hat{r}_i)}{kT_s}\right).$$

(14c)

Many researchers have worked on the problem of hard sphere solutes distributing between a bulk phase and another phase containing other fixed hard spheres.[23,25,26] We follow the work of Rikvold and Stell,[26] where they have formulated the partitioning coefficient, K_n, for hard spherical (dilute) solutes partitioning between bulk phase and a phase constituted of disordered hard spheres. This work is based upon Torquato's[25] concentric-shell model, which, briefly, visualizes the porous medium as a disordered distribution of spheres of diameter a and a *hardness parameter* δ (which lies in the range [0,1], depending upon the degree of *penetrability* of the spheres). In the present case, we have the brush phase constituted of totally impenetrable polymer segments and hence $\delta = 1$. The only constraint upon the results of the concentric shell model is that the probability of any two sphere centers approaching closer than δa is zero. Rikvold

and Stell generalize the model to obtain the specific volume and the specific surface area available to a probe particle of a finite size. The partition coefficient for a finite sized hard solute ($\hat{r}_i \neq 0$) is then defined as the ratio of the pore volume accessible to the finite solute to that accessible to a point solute ($\hat{r}_i = 0$). Rikvold and Stell give the partition coefficient, K_n, for a solute of radius $\hat{r}_i$ as[23]

$$K_n = \left[\exp\left(-\frac{\Phi}{1-\Phi}\right)\right]^{C(\hat{r}_i)},$$

(15)

where, $C(\hat{r}_i)$ is given by the following expression:

$$C(\hat{r}_i) = 3\left[\hat{r}_i + \tfrac{1}{2}\left(\frac{3}{1-\Phi} - 1\right)\hat{r}_i^2 \right.$$
$$\left. + \left(\frac{1}{(1-\Phi)^2} - \frac{1}{1-\Phi} + \frac{1}{3}\right)\hat{r}_i^3\right].$$

(16)

Comparison of Eq. (16) with Eq. (14c) leads to the following expression for the ion excluded volume energy, g_i:

$$\frac{g_i}{kT_s} = C(\hat{r}_i)\left(\frac{\Phi}{1-\Phi}\right).$$

(17)

Equation (17), when combined with Eq. (13), allows one to express the concentration of the ions in the voids in terms of the electrostatic potential and the local segment volume fraction. However, the quantity of interest in our mean field picture is the concentration of the ions over the *total* volume (the sum of the voidage and the space occupied by the segments). This quantity, n_i, simply equals

$$n_i = n_i^\infty(1-\Phi)\exp\left\{-\frac{Z_i e\Psi}{kT_s} - C(\hat{r}_i)\left(\frac{\Phi}{1-\Phi}\right)\right\}.$$

(18)

It is worthwhile noting that, even for point charges, if the polymer volume fraction is unity, the preexponential factor on the right-hand side of Eq. (18) forces the ion concentration to vanish in the brush. Thus, this representation leads to a consistent description of the ion distribution in the brush.

One can also note that in the Henry law regime, where the above expression is valid, one is justified in making the following approximation:

$$\Phi_{\text{solvent}} \approx 1 - \Phi.$$

(19)

In such a case, one would expect the segments to have excluded volume interactions predominantly with each other and with the solvent. The contribution of the ions to the excluded volume free energy of the *segments* can then be neglected. One can easily verify that in many realistic systems, such an assumption would not constitute a gross approximation. For example, consider a 1:1 electrolyte solution of 0.1 M concentration, both ions being 5 Å in radius (To illustrate that this number is typical, compare it with the following radii: K^+, Cl^-, $NO3^- \sim 0.35$ nm, $Na^+ \sim 0.45$ nm and $H^+ \sim 0.9$ nm). The volume fraction of each type of ion is about 0.03, which is an order of magnitude smaller than that of the polymer (~ 0.3). In most cases, therefore, for ionic sizes $\leqslant 5$ Å and/or ionic strengths $\leqslant 0.1$ molar, we expect that this assumption will provide reasonable answers to the polyelectrolyte brush problem.

This model does not also include any specific ion–polymer or ion–solvent interactions; only hard core and electrostatic interactions are accounted for. One can also use other approaches for formulating the nonelectrostatic energy of the ions, g_i, including Flory–Huggins type of expressions for the free energy of the ions.[27,28] Here the Flory–Huggins parameters χ_{ij} could be related to the excluded volume interactions of the ions. The hard core model, however, with the assumptions involved in Eq. (18), does provide a simple and tractable picture of the ion-size effect. In particular, the only other parameter defining the ions, apart from the charge, is their hard sphere diameter. This makes the model easy to visualize when comparing the ionic size to the size of the voids in the polymer brush.

IV. POLYELECTROLYTE BRUSH MODEL

The approach to solving the polyelectrolyte brush problem follows as before (Ref. 20), by equating the total potential of Eq. (8), to the sum of the electrostatic and nonelectrostatic parts of the segment potential.

We adopt the Flory–Huggins expression for nonelectrostatic part of the segment potential. Keeping in mind that the ionic solution is dilute [see Eq. (19)], we can write the nonelectrostatic part of the segment potential as

$$W_n = -\ln(1 - \Phi) - 2\chi\Phi, \qquad (20)$$

and the electrostatic part of the segment potential as

$$W_e = \frac{\alpha Z_p e \Psi}{kT_s}. \qquad (21)$$

The total segment potential can, therefore, be written as

$$A(h) - U(x) = [W_n(x) + W_e(x)]$$

$$= -\ln(1 - \Phi) - 2\chi\Phi + \frac{\alpha Z_p u}{Z}. \qquad (22)$$

In the above equations χ is the Flory–Huggins interaction parameter for the polymer and solvent pair. Z is the valence of the Z:Z electrolyte and u is the dimensionless electrostatic potential equal to $Ze\Psi/kT_s$. α is the degree of dissociation of the segments and is assumed to be spatially invariant.

The electrostatic potential distribution is governed by the Poisson–Boltzmann equation. The Poisson–Boltzmann equation is written separately for the region inside the brush and the region outside the brush, which is devoid of any polymer segments.

Inside the brush region, the equation takes the following form:

$$\frac{d^2u^{(i)}}{dx^2} = -\frac{4\pi Zea^2}{\epsilon kT_s}\left[Ze(n_+ - n_-) + \frac{\alpha Z_p e\Phi}{v_s}\right], \quad x \leqslant h^*, \qquad (23)$$

the superscript, (i), referring to the inner region. Here, n_+ and n_- are the concentrations of the cation and anion, respectively, given by Eq. (18). These concentrations depend upon the ion size (which may be different for cations and anions, in general) and upon the local segment density.

Outside the brush region we have,

$$\frac{d^2u^{(o)}}{dx^2} = -\frac{4\pi Z^2e^2a^2}{\epsilon kT_s}(n_+ - n_-), \quad x > h^*, \qquad (24)$$

the superscript, (o), referring to the outer region and the superscript "$*$" referring to the equilibrium brush height. In the outside region, having no polymer segments, the nonelectrostatic ion potential, g_i, of the ions uniformly vanishes and the ionic concentrations depend only upon the electrostatic potential, as given by Eq. (10). The solution to the electrostatic potential distribution in the outside region is known from Guoy–Chapman theory as

$$\tanh\left(\frac{u}{4}\right) = \tanh\left(\frac{u(x = h^*)}{4}\right)\exp(-\kappa ax). \qquad (25)$$

Here, κ is the inverse of the debye screening length defined as $(8\pi Z^2e^2n_\infty/\epsilon kT_s)^{1/2}$.

By requiring the electrostatic potential and its derivative to be continuous at the brush height, we can write down the following boundary condition for the electrostatic potential distribution inside the brush.

$$\frac{du^{(i)}}{dx} = -2a\kappa\sinh\left(\frac{u^{(i)}}{2}\right), \quad x = h^*. \qquad (26)$$

The boundary condition for the electrostatic potential at the surface is related to the surface charge, σ_0, as follows:

$$\frac{du^{(i)}}{dx} = -\frac{4\pi Zea\sigma_0}{\epsilon kT_s}, \quad x = 0. \qquad (27)$$

Thus, the electrostatic potential needs to be solved only inside the brush region now. The whole problem can now be defined in the form of four first order differential equations whose solution will provide the self-consistent-field picture of the polymer brush. We use the following designations, in order to write the equations and the boundary conditions, in a computationally convenient fashion: $Y_1 \equiv U$, $Y_2 \equiv \Phi$, $Y_3 \equiv u^{(i)}$, and $Y_4 \equiv du^{(i)}/dx = u^{(i)'}$.

Differentiating Eq. (9) and inverting both sides, one can write,

$$\frac{dY_1}{dx} = \frac{1}{N\sqrt{\frac{2}{\pi}}}\left[\frac{1}{\sqrt{\pi Y_1}} - \sqrt{\frac{2}{\pi}}\right.$$

$$\left.\exp\left(\frac{2Y_1}{\pi}\right)\text{erfc}\left(\sqrt{\frac{2Y_1}{\pi}}\right)\right]^{-1}$$

$$= j(Y_1). \qquad (28)$$

Differentiating Eq. (22), one can write,

$$\frac{dY_2}{dx} = j(Y_1) + \frac{\alpha Z_p Y_4}{Z}\bigg/\left(2\chi - \frac{1}{1 - Y_2}\right). \qquad (29)$$

The Poisson–Boltzmann equation may be written as two first order equations,

$$\frac{dY_3}{dx} = Y_4, \qquad (30)$$

$$\frac{dY_4}{dx} = -\frac{4\pi Zea^2}{\epsilon kT}\left[Ze(n_+ - n_-) + \frac{\alpha Z_p e Y_2}{v_s}\right], \qquad (31)$$

keeping in mind that $n_i \equiv n_i(Y_2, Y_3, \hat{r}_i)$, as given by Eqs.

(16) and (18). Here $v_s = \pi a^3/6$. The boundary conditions are as follows:

The variable part of the segment potential, U, vanishes at the surface [see Eq. (9)], or

$$x = 0, \quad Y_1 = 0. \tag{32}$$

The segment density is required to vanish at brush height for an equilibrium brush

$$x = h^*, \quad Y_2 = 0. \tag{33}$$

The electrostatic potential at the surface is related to the surface charge, σ_0, or

$$x = 0, \quad Y_4 = -\frac{4\pi Zea\sigma_0}{\epsilon k T_s}, \tag{34}$$

and at the top of the brush,

$$x = h^*, \quad Y_4 = -2\kappa a \sinh\left(\frac{Y_3}{2}\right). \tag{35}$$

Any self-consistent solution for the segment density and electrostatic potential profiles must be governed by Eqs. (28)–(31) and must satisfy the boundary conditions (32)–(35).

The grafting density, σ, and the chain length, N, being known, the segment density distribution obtained after solving the above equations should satisfy the following constraint:

$$\frac{N\sigma v_s}{a} = \int_0^{h^*} dx\, \Phi(x). \tag{36}$$

The brush height h^* is unknown at the outset. One starts by making an initial guess for the brush height and solving the above equations. The error in satisfying the constraint, i.e., Eq. (36), is used to find a better estimate of the brush height, h^*. An iterative procedure is followed until the constraint is satisfied and the solution for the segment density distribution is obtained.

A. Free energy of the chains in the brush

Once the solution of the above equations is known, one can compute the constant $A(h)$ appearing in the expression for $W(x)$.

$$A(h) = W(0) = -\ln[1 - \Phi(0)] - 2\chi\Phi(0) + \alpha\frac{Z_p}{Z} u(0) \tag{37}$$

This is nothing but the potential of a segment in contact with the surface. This potential is uniquely determined for a given grafting density, σ, and therefore $A \equiv A(\sigma)$. The free energy, S_i, of any arbitrary (ith) chain in the brush is the same as that of the chain lying at the surface.

$$S_i = NA(\sigma). \tag{38}$$

The free energy (per chain) in the brush, $\mathscr{F}$, can therefore be written as (see Refs. 15 and 18 for further details),

$$\mathscr{F} = \frac{N}{\sigma} \int_0^{\sigma} d\sigma' A(\sigma'). \tag{39}$$

V. RESULTS AND DISCUSSION

In the following section, we present some salient results concerning the effect of the finite extensibility and finite size of the ions. The following are some of the main parameters which are constant throughout the computations: chain length, $N = 1000$, segment size, $a = 1$ nm, grafting density, $\sigma = 10^{17}$ m^{-2} ($\sim 10\%$ coverage), surface charge density, $\sigma_0 = 0$, ion valance, $Z = 1$, segment valence, $Z_p = -1$, and Flory–Huggins parameter, $\chi = 0.45$. The solvent is water at 298 K. The volume of the segments is $v_s = \pi a^3/6 = 5.24 \times 10^{-28}$ m^3. It may be noted that the regime chosen for this study envisages brushes immersed in a good solvent where ionic strengths are low. Under all circumstances, therefore, one would expect the "effective" solvent to be a good one and either microphase or macrophase separation is not expected.[29]

The dimensionless coordinate, x, perpendicular to the wall, is scaled by the dimensionless chain length N in order to obtain a new variable $\xi(=x/N)$. In all figures, distances are depicted by this new variable. ξ^* denotes the height of an equilibrium brush and $\xi = 1$ corresponds to a fully stretched chain.

In order to focus on each of the two proposed extensions, viz., finite extensibility and the finite ion size, we break up the discussion of the results into two subsections. In subsection V A, we will assume the ions to be point charges and concentrate on the finite extensibility of the chains alone. In subsection V B, we present the results which account for the finite ion size as well as finite extensibility.

A. Finite extensibility of the chains

In the first three figures, we concern ourselves with the effect of the finite extensibility correction only. Assuming that the ions are point charges, we study the effect of the backbone charge density, characterized by α, and ionic strength, I, upon the equilibrium segment density distributions and the brush heights.

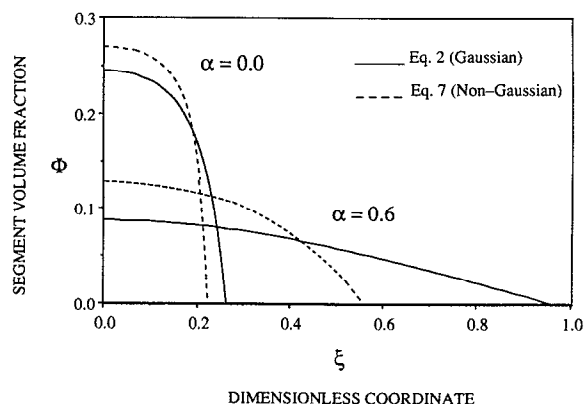In Fig. 1, two segment density distributions are depicted

FIG. 1. The effect of accounting for the finite extensibility of polymer chains on the segment density distributions. Grafting density, $\sigma = 10^{17}$ m^{-2}, chain length, $N = 1000$, segment size, $a = 1$ nm, solvent quality, $\chi = 0.45$, segment valence, $Z_s = -1$, electrolyte valence, $Z = 1$, surface charge density, $\sigma_0 = 0.0$, ionic strength, $I = 0.1$ M, ionic radii, $\hat{r}_+ = \hat{r}_- = 0.0$.
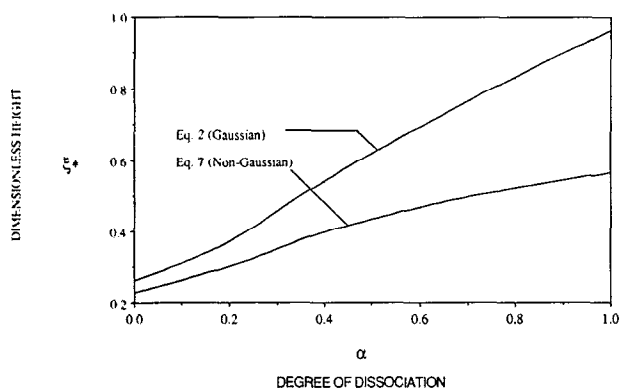
FIG. 2. The effect of accounting for the finite extensibility of polymer chains on the brush height. The brush height is studied as a function of backbone charge density. Grafting density, $\sigma = 10^{17}$ m^{-2}, chain length, $N = 1000$, segment size, $a = 1$ nm, solvent quality, $\chi = 0.45$, segment valence, $Z_s = -1$, electrolyte valence, $Z = 1$, surface charge density, $\sigma_0 = 0.0$, ionic strength, $I = 0.1$ M, ionic radii, $\hat{r}_+ = \hat{r}_- = 0.0$.

at two different values of backbone charge density. The SDDs are shown assuming both the Gaussian [Eq. (2)] and the corrected [Eq. (7)] forms for the stretch energy. In the case where the finite extensibility has been accounted for, we have already noted that the segment potential drops very rapidly compared to the Gaussian elasticity case. Therefore, the chains in the non-Gaussian (corrected) case are not stretched nearly as much as would be predicted by the Gaussian elasticity term. This leads to a contraction in the SDDs which drop more steeply. The variance in the predictions of the Gaussian and corrected cases increases with higher backbone charges. This follows from the fact that the higher charge stretches the chains more, increasing, thereby, the importance of the finite extensibility correction.

Figure 2 compares the brush height predictions for the two cases (Gaussian and corrected) as a function of the backbone charge. The corrected version of the elastic term leads to smaller brush heights, again by virtue of the steeper potential. Indeed, as expected, the difference in the predic-
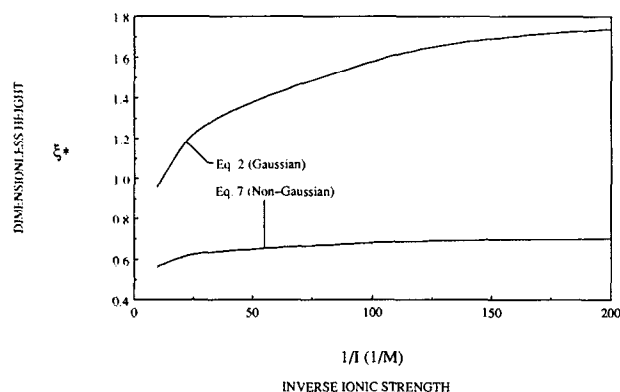
tions increases at high charges due to higher stretching of the chains.

In Fig. 3, the brush heights are compared for various values of ionic strength. Lower ionic strength leads to lesser screening of the segmental charges and therefore to higher repulsion amongst the segments. Thus, the stretching of the chains increases with lowering of the ionic strength. As expected, we again find lower brush height predictions for the corrected stretch case. The discrepancy in the predictions of the Gaussian and the non-Gaussian cases increases with lowering ionic strength, due to increased intersegmental repulsions. The interesting fact that emerges from this figure is that not accounting for the finite extensibility corrections can lead to brush height predictions which exceed the chain length ($\xi^* \geqslant 1$).

The finite extensibility corrections are thus very important for polyelectrolytes. Even at the relatively low surface coverage ($\sim 10\%$ here), high stretching is induced in the chains due to electrostatic repulsions. This would necessitate accounting for the finite extensibility corrections for polyelectrolytes under most commonly encountered situations. The finite extensibility correction would, of course, vary from one polymer to the other and, therefore, the stretch rates at which these corrections become significant would also vary. Whatever the relevant stretch representation for a given polymeric species, as long as it satifies the constraints imposed by Eqs. (4a) and (4b), the segment potential would drop steeper within the brush compared to the Gaussian case.

B. Finite size of the added electrolyte ions

Having accounted for the finite extensibility corrections, we now focus upon the effect of varying the size of the electrolyte ions. In the following figures, we explore the effect of changing the size of the co-ions (electrolyte ions with the same sign as the segment charge) and the counterions (electrolyte ions with a sign opposite to the segment charge) on the brush structure.

In Fig. 4, keeping the size of the co-ion fixed, the size of the counterion is increased. The brush height, ξ^*, increases
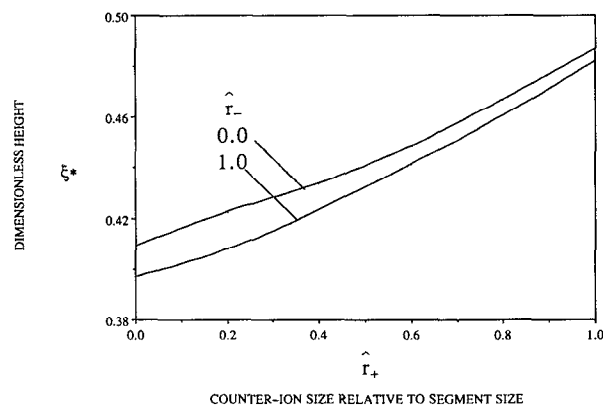

FIG. 3. The effect of accounting for the finite extensibility of polymer chains on the brush height. The brush height is studied as a function of the ionic strength for a constant degree of dissociation, $\alpha = 1$. Grafting density, $\sigma = 10^{17}$ m^{-2}, chain length, $N = 1000$, segment size, $a = 1$ nm, solvent quality, $\chi = 0.45$, segment valence, $Z_s = -1$, electrolyte valence, $Z = 1$, surface charge density, $\sigma_0 = 0.0$, ionic radii, $\hat{r}_+ = \hat{r}_- = 0.0$.

COUNTER-ION SIZE RELATIVE TO SEGMENT SIZE

FIG. 4. The effect of the varying size of the counterions on brush height. The co-ion size is fixed. Grafting density, $\sigma = 10^{17}$ m^{-2}, chain length, $N = 1000$, segment size, $a = 1$ nm, solvent quality, $\chi = 0.45$, segment valence, $Z_s = -1$, $\alpha = 0.4$, electrolyte valence, $Z = 1$, surface charge density, $\sigma_0 = 0.0$, ionic strength, $I = 0.1$ M.
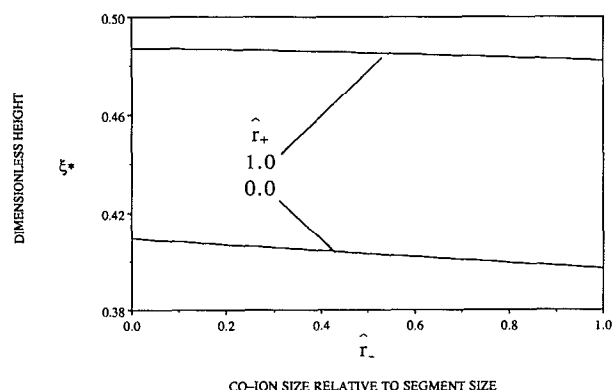
FIG. 5. The effect of the varying size of the co-ions on brush height. The counterion size is fixed. Grafting density, $\sigma = 10^{17}$ m^{-2}, chain length, $N = 1000$, segment size, $a = 1$ nm, solvent quality, $\chi = 0.45$, segment valence, $Z_s = -1$, $\alpha = 0.4$, electrolyte valence, $Z = 1$, surface charge density, $\sigma_0 = 0.0$, ionic strength, $I = 0.1$ M.
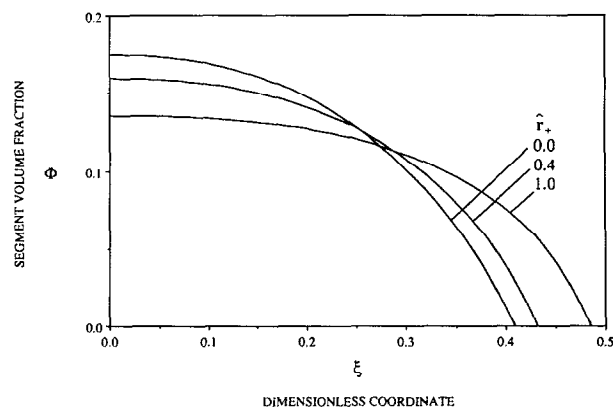

FIG. 6. The effect of the varying size of the counterions on the segment density distribution. The co-ion size is fixed (point charge). Grafting density, $\sigma = 10^{17}$ m^{-2}, chain length, $N = 1000$, segment size, $a = 1$ nm, solvent quality, $\chi = 0.45$, segment valence, $Z_s = -1$, $\alpha = 0.4$, electrolyte valence, $Z = 1$, surface charge density, $\sigma_0 = 0.0$, ionic strength, $I = 0.1$ M, ionic radius $\hat{r}_- = 0.0$.

with increasing counterion size. This can be explained in terms of the nonelectrostatic energy, g_i, of the counterions. As the size of the ion increases, its nonelectrostatic energy increases too, according to Eqs. (16) and (18). This increase in the nonelectrostatic energy leads to a reduction in their concentration inside the brush. It is, however, the counterions that are responsible for shielding the segments from mutual electrostatic repulsion. As the counterion size increases, and their concentration in the brush decreases, the higher intersegmental repulsion forces the segments apart, leading to higher brush heights.

In Fig. 5, the situation is reversed; the counterion size is constant while the co-ion size is allowed to vary. It is expected, by earlier arguments, that as the co-ion size increases, their concentration would decrease inside the brush. This inability of the co-ions to pervade the brush would make the counterions more effective in screening the segment–segment electrostatic repulsion. As a result, one observes smaller brush height with larger co-ions. This is, indeed, observed in Fig. 5, although the effect is much smaller (compared to the changes caused by counterion size variation). This is expected as most of the co-ions are forced out of the brush region by unfavorable electrostatic potential, i.e., their concentration inside the brush is small to begin with. Therefore, increasing their nonelectrostatic energy decreases their concentration only marginally.

Figure 6 depicts the segment density distributions for different counterion sizes. The segment density distributions are more spread out with increasing counterion size. This again follows from the arguments that apply to Fig. 4, viz., increase in size leads to decrease in counterion concentration and hence more intersegmental repulsions.

Finally, in Fig. 7 the free energy of the brush, as a function of the ion sizes, is shown. The brush can be visualized as being formed by bringing polymer chains, one by one, to the grafting surface, until the required grafting density is obtained. In the course of brush formation, larger counterions are excluded, from the evolving brush, due to their size. This increases the electrostatic potential in the brush region.

Thus, more "work" needs to be done to bring more chains to the surface. This appears as the increase in the free energy of the brush with increasing counterion size, as shown in Fig. 7. By the same argument, increased co-ion size leads to their exclusion from the brush region, thus lowering the electrostatic potential. The result is that brush free energy decreases with increasing co-ion size. However, as noted earlier, this decrease is relatively negligible since the co-ion concentrations in the brush are low to begin with.

It thus appears from these results that everything else in the system held the same, changing the electrolyte (and hence the ion size) would change the brush conformations. The interaction between surfaces carrying polyelectrolytes would also, therefore, be different if the electrolyte were to be different. For a larger counterion size, we might expect larger repulsive forces (due to higher electrostatic potentials) which operate at a larger distance (due to higher brush height).
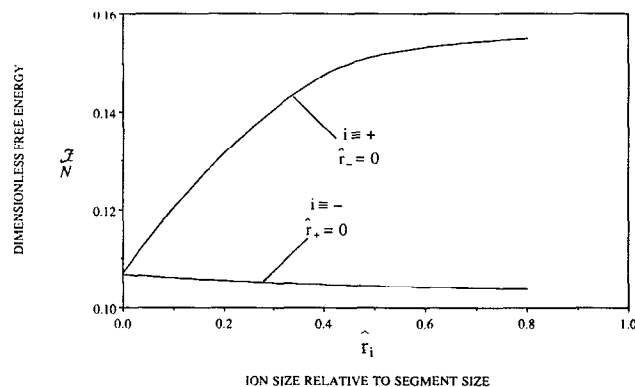

FIG. 7. The effect of the varying size of the ions on the free energy of the brush. Grafting density, $\sigma = 10^{17}$ m^{-2}, chain length, $N = 1000$, segment size, $a = 1$ nm, solvent quality, $\chi = 0.45$, segment valence, $Z_s = -1$, $\alpha = 0.2$, electrolyte valence, $Z = 1$, surface charge density, $\sigma_0 = 0.0$, ionic strength, $I = 0.1$ M.

The changes in the brush structure due to ion size changes are significant. This applies especially to the counterion size, which makes a sizable difference to the structure and free energy of the brush. The co-ion size change, by contrast, changes the brush properties only in a minor fashion. It should be noted that the magnitude of the ion-size effect depends upon the grafting density (or segment density distribution) of the polymer as well. The finite size of the ions should make a bigger difference for more dense brushes. In other words, for more dense brushes even smaller ions will have significant excluded volume interactions with the polymer layer.

VI. CONCLUSIONS

Two effects, hitherto unaccounted for, that affect polymer brush structure are explored. One of these is the effect of the finite extensibility of the chains, which limits the stretching rate of the chains. While the magnitude of this effect varies from polymer to polymer, it results in a steeper segment potential profile and constrains the brush height to remain less than the chain length. The other effect, that of accounting for the excluded volume energy of the ions, is also quite significant. Increased ion-size decreases the ion concentration in the brush region due to their increased excluded volume energy. Increasing counterion size, therefore, leads to greater intersegmental repulsions and hence larger brush heights and free energies. The co-ion size variation, by contrast, makes only a minor impact upon brush properties. The range and the magnitude of the repulsive forces between surfaces carrying polyelectrolyte brushes could also be expected to increase by increasing the counterion size. While the ion-size effect is important for brushes, one expects it to play an important role for the case of adsorbed homopolymers as well.

ACKNOWLEDGEMENT

APPENDIX: THE EQUAL TIME POTENTIAL

The following is the approach is outlined by Shim and Cates[21] in order to obtain an equal time potential for a given finite extensibility correction. One can use the classical mechanics analogy, that the sum of kinetic (or stretch) energy and the potential (or interaction) energy, say H, should be constant for a particle moving in a conservative field. One can obtain H as follows:

$$H = \dot{x} \frac{\partial L}{\partial \dot{x}} - L, \qquad (A1)$$

where L, the Lagrangian, is the sum of the stretch and interaction energies, or

$$L(\dot{x}, x, n) = T + W. \qquad (A2)$$

This constant of motion, H, can be chosen as the potential (or interaction) energy of the particle when it is at rest (i.e., the interaction potential of the segment at the free end of the polymer). This can be, say, $W(\zeta)$ for a chain whose

free end is at $x = \zeta$. Equating $H = W(\zeta)$, one can get a relation of the form,

$$\dot{x} = \frac{1}{P[W(\zeta) - W(x)]} = \frac{1}{P[U(\zeta) - U(x)]}$$
$$= \frac{1}{P(\Delta U)}. \qquad (A3)$$

If all chains are of equal length, then the equal time constraint requires that all "particles" take the same "time" to reach the surface no matter where they start from. In other words, one can write, using a transformation from $x \rightarrow U$,

$$N = \int_0^\zeta \frac{dx}{\dot{x}} = \int_0^U dU' \, j(U') P(U - U'), \qquad (A4)$$

where, $j(U) = dx/dU$. One can obtain the Laplace transform, $U \rightarrow s$, of this equation as,

$$\mathcal{L}\{j(U)\} = \frac{N}{s \mathcal{L}\{P(U)\}}. \qquad (A5)$$

It is now possible to obtain the inverse transform of this equation and obtain the derivative of U. The derivative can be integrated using the condition $x = 0$, $U = 0$, to obtain the equal time potential. The success of this technique in obtaining easily tractable solutions depends much upon obtaining expressions of the type (A3). In addition, one must find the Laplace transform of this expression (A4) and the inverse of equation (A5)—both of which must be obtainable easily.

NOMENCLATURE

a The diameter of the spherical segment (or segment size).
A The constant part of the segment interaction potential profile, W.
B A constant, characteristic of the parabolic potential. It equals $\pi^2/8N^2$.
$C(\hat{r}_i)$ A constant appearing in the nonelectrostatic part of the free energy of the ith ionic specie, given by Eq. (17).
e The protonic charge, 1.6×10^{-19} C.
g_i The local nonelectrostatic free energy of the ith ionic species (arising from volume exclusion).
h^* The height of an equilibrium brush dedimensionalized by the segment size, a.
H A constant characterizing the interaction potential of the free segment on a chain.
H_i A constant characterizing the interaction potential of the free segment of the ith chain.
j The negative of the gradient of the segment interaction potential profile, W.
k The Boltzmann constant. 1.38×10^{-23} J K^{-1}.
K The coefficient of partition for spherical solutes between the bulk and a matrix made up of disordered hard spherical obstacles.
L Lagrangian of a chain in the brush, defined as $(T + W)$.
L_i Lagrangian of the ith chain in the brush, defined as $(T_i + W_i)$.
n_+ The local concentration of the positive ions of the $Z:Z$ symmetric electrolyte.
n_- The local concentration of the negative ions of the $Z:Z$ symmetric electrolyte.

n^{∞} The bulk concentration of the Z:Z symmetric electrolyte.

n_i The local concentration of the ith ionic specie.

n_i^p The local concentration of the ith ionic species in the "interstitial" region of the brush (i.e., the fraction of the space unoccupied by the polymer segments).

n_i^{∞} The bulk concentration of the ith ionic species.

N The number of segments in each chain. Also the chain length dedimensionalized by the segment size, a.

r_i The radius of the ith ionic species which is assumed to be a hard, spherical entity.

$\mathbf{r}_i$ (s) The coordinate of the sth segment in the ith chain.

$\hat{r}_i$ The radius of the ith ionic species dedimensionalized by the segment size, a.

r_p The local hydraulic radius of the "interstitial" region in the brush (i.e., the fraction of the space unoccupied by the polymer segments).

s The ranking of the segment referenced from the free end of the chain.

S_i The action of the ith chain.

T The local stretching rate of a chain in the brush.

T_i (s) The stretch (or entropy) part of the free energy of the sth segment of the ith chain.

T_s The absolute temperature of the system.

u The nondimensional electrostatic potential, given as $Ze\Psi/kT_s$.

U The space dependent part of the segment interaction potential profile, W.

v_s The volume of the polymer segments $(\pi a^3/6)$.

W The interaction potential of a segment in the brush.

W_e The electrostatic part of the segment interaction potential profile, W.

W_n The nonelectrostatic part of the segment interaction potential profile, W.

W_i (s) The interaction potential of the sth segment of the ith chain.

x The distance from the grafting surface dedimensionalized by the segment size, a.

$\dot{x}$ The local stretching rate of a chain $\partial x/\partial s$.

$\dot{x}_i$ (s) The stretching rate $\partial x_i/\partial s$ of the sth segment of the ith chain.

Y_1 Equivalent to U.

Y_2 Equivalent to Φ.

Y_3 Equivalent to u.

Y_4 Equivalent to the gradient of u, $\partial u/\partial x$.

Z The valence of a Z:Z, symmetric electrolyte.

Z_i The valence of the ith ionic species.

Z_p The valence of the polymer segments.

Greek symbols

α The degree of dissociation of the dissociable groups on the segments.

χ The Flory–Huggins interaction parameter.

δ Hardness parameter for spheres constituting the random two phase medium.

ϵ The dielectric constant of the solvent.

Φ The local segment volume fraction.

$\mathscr{F}$ Free energy of a system of grafted chains, per unit grafting surface area.

κ The reciprocal of the Debye screening length. $(\kappa^2 = 8\pi Z^2 e^2 n^{\infty}/\epsilon kT_s)$.

σ The density of the grafted chains per unit surface area.

σ_0 The surface charge density on the grafting plane.

ξ The distance from the surface dedimensionalized by the chain length, $(\xi = x/N)$.

ξ^* The equilibrium brush height dedimensionalized by the chain length, $(\xi^* = h^*/N)$.

Ψ The local electrostatic potential.

[1] H. J. Tauton, C. Toprakcioglu, L. J. Fetters, and J. Klein, Nature 332, 712 (1988).

[2] G. Hadziioannou, S. Patel, S. Granick, S. and M. Tirrell, J. Am. Chem. Soc. 108, 2869 (1986).

[3] B. A. Costello, P. F. Luckham, and T. F. Tadros, Colloid Surf. 34, 301 (1989).

[4] D. H. Napper, Polymeric Stabilization of Colloidal Dispersions (Academic, New York, 1972).

[5] T. A. Witten and P. A. Pincus, Macromolecules 19, 2509 (1986).

[6] P. A. Pincus, Macromolecules, 24, 2912 (1991).

[7] J. T. Kim and J. L. Anderson, J. Membr. Sci. 47, 163 (1989).

[8] S. Misra and S. Varanasi, J. Colloid Interface Sci. (in press).

[9] J. Noolandi and K. M. Hong, Macromolecules 16, 1443 (1983).

[10] M. R. Munch and A. P. Gast, Macromolecules 21, 1360 (1988).

[11] Ed. L. H. Lee, New Trends in Physics and Physical Chemistry of Polymers (Plenum, New York, 1989).

[12] Polymer Surfaces and Interfaces edited by W. J. Feast and H. S. Munro (Wiley, New York, 1987).

[13] S. J. Alexander, J. Phys. France 38, 983 (1977).

[14] P. G. deGennes, Adv. Colloid Interface Sci. 27, 189 (1987).

[15] T. Cosgrove, T. Heath, B. van Lent, F. Leermakers, and J. Scheutjens, Macromolecules 20, 1692 (1987).

[16] S. Hirz, thesis, University of Minnesota, 1987.

[17] J. S. Ho and M. Muthukumar, Macromolecules 22, 965 (1989).

[18] S. T. Milner, T. A Witten, and M. E. Cates, Macromolecules 21, 2610 (1988), and references therein.

[19] S. J. Miklavic and S. Marcelja, J. Phys. Chem. 92, 6718 (1988).

[20] S. Misra, S. Varanasi, and P. P. Varanasi, Macromolecules 22, 4173 (1989), and references therein.

[21] D. F. K. Shim and M. E. Cates, J. Phys. France 50, 3535 (1989), and references therein.

[22] P. G. de Gennes, Rep. Prog. Phys. 32, 187 (1969).

[23] P. A. Rikvold and G. Stell, J. Colloid Interface Sci. 108, 158 (1985).

[24] J. Koryta and J. Dvorak, Principles of Electrochemistry (Wiley, New York, 1987).

[25] S. Torquato, J. Chem. Phys. 81, 5079 (1984).

[26] L. A. Fanti, E. D. Glandt, and W. G. Madden, J. Chem. Phys. 93, 5945 (1990).

[27] D. E. Brooks, J. Colloid Interface Sci. 43, 687 (1973).

[28] M. R. Bohmer, O. A. Evers, and J. M. H. M. Scheutjens, Macromolecules 23, 2288 (1990).

[29] If one considers a polyelectrolyte solution in a bad solvent, increasing the electrolyte concentration may decrease the "effective" solvent quality. In such a case, first a microphase and subsequently, upon addition of more electrolyte, a macrophase separation might occur. For example, refer to V. Yu. Borue and I. Ya. Erukhimovich, Macromolecules 21, 3240, (1988).